Proceedings of the Estonian Academy of Sciences,
2013, **62**, 2, 97–108
doi: 10.3176/proc.2013.2.03
Available online at www.eap.ee/proceedings

PHYSICS

Numerical study of upward particulate pipe flows at a constant Reynolds number

Alexander Kartushinsky, Ylo Rudi*, Sergei Tisler, Igor Shcheglov, and Alexander Shablinsky

Research Laboratory of Multiphase Media Physics, Faculty of Science, Tallinn University of Technology, Akadeemia tee 15A, 12618 Tallinn, Estonia

Received 27 October 2011, accepted 13 November 2012, available online 7 May 2013

Abstract. The method based on 2D Reynolds-averaged Navier–Stokes equations has been employed for the simulation of upward turbulent particulate cylindrical pipe flows of different diameters for a constant flow Reynolds number. This approach was supplied with appropriate closure equations which took into account all pertinent forces and effects that exerted influence on gas and particles: the particle–particle, particle–wall, and particle–turbulence interactions; gravitation, viscous drag, and lift forces; and turbulence modulation. The finite volume technique was applied to the numerical solution of the governing equations. The results show the effect of the mass loading on the radial distributions of the longitudinal velocity lag, the turbulence modulation, and particle concentration. In particular, the two-way coupling of turbulence with the given particles raises simultaneously the velocity lag between gas and particles, originating from direct impact of turbulence on particle motion, and turbulence attenuation by the particles. The radial distributions of longitudinal particle velocity and mass concentration become flatter for higher flow mass loading.

Key words: vertical pipe, particulate flow, terminal velocity, turbulence modulation, flow mass loading.

INTRODUCTION

Particulate flows in pipes have numerous engineering applications ranging from pneumatic conveying systems to coal gasifiers and chemical reactor design and are one of the most thoroughly investigated subjects in the area of multiphase flows. These flows are very complex and influenced by various physical phenomena, such as particle–turbulence and particle–particle interactions, deposition, by gravitational and viscous drag forces, particle rotation, and lift force.

Numerous theoretical and experimental researches (e.g. Pfeffer et al., 1966; Tsuji and Morikawa, 1982; Michaelides, 1983, 2006; Tsuji et al., 1984; Davies, 1987; Gore and Crowe, 1989; Squires and Eaton, 1990; Yuan and Michaelides, 1992; Cabrejos and Klinzing, 1994; Gidaspow, 1994; Yarin and Hetsroni, 1994; Cao and Ahmadi, 1995; Crowe and Gillandt, 1998; Crowe, 2000; Sommerfeld, 2003; Kartushinsky and Michaelides, 2004; Kartushinsky et al., 2009a, 2009b, 2011) deal with various aspects of the behaviour of gas and solid particles in particulate pipe flows.

The present study focuses on the effect of variation of the pipe diameter for a constant Reynolds number applied to vertical particulate turbulent pipe flows. The numerical investigation discussed here examined in detail the effects of direct and indirect particle–turbulence interaction (no-coupling and coupling) and gravity for various flow mass loadings. Additionally, the viscous drag force and the Magnus and Saffman lift forces are also taken into account. The presented numerical model makes use of the two-

* Corresponding author, ulo.rudi@ttu.ee

fluid model (Elghobashi and Abou-Arab, 1983; Rizk and Elghobashi, 1989; Deutsch and Simonin, 1991; Simonin, 1991; Reeks, 1992) and the Reynolds-averaged Navier–Stokes (RANS) approach (Kartushinsky et al., 2009a, 2009b) applied to gas and solid particles.

Within the frame of the two-fluid model, the gas and the particles are considered as two coexisting phases that span the entire flow domain (Kartushinsky et al., 2009a, 2009b). Therefore, in order to describe the flow of the particulate phase within the two-fluid model, the presented model implements the RANS approach. This approach is the most general and frequently used in modelling, its closure equations have been verified by numerous experiments, and the boundary conditions are easy to determine. The given modelling employs the model by Crowe (2000). It is the most relevant model to account for mechanisms of a turbulence modulation caused by particles, since it includes both the turbulence enhancement and its attenuation by particles. The inter-particle collisions are another mechanism accounting for capture properties of turbulent particulate pipe flows, which has been modelled, e.g., by Kartushinsky and Michaelides (2004). These two models enable comprehensive mathematical simulation of the two-phase upward pipe flow.

The presented model allows covering 100 and more calibers of a pipe flow. This is the main advantage over the numerical models based, for example, on direct numerical simulation codes (e.g., Marchioli et al., 2003), that handle usually with a short pipe length up to 10–20 calibers with imposing the upper limit for the flow Reynolds number.

The utilized two-fluid model with adoption of the original collisional closure model by Kartushinsky and Michaelides (2004) together with the applied numerical method has been verified and validated in our previous research (Kartushinsky et al., 2009a, 2009b) by comparison of numerical results with the existing experimental data by Tsuji et al. (1984). In the given study, the effect of variation of the pipe diameter (or transport velocity) at a constant Reynolds number is numerically investigated in the particulate turbulent flow. This is a step forward for analysing the external effect, namely, the flow configuration rather than the internal effect with variation of the parameters of the flow.

MATERIALS AND METHODS

Model description

The sketch of the computational flow domain is shown in Fig. 1, where $\overline{u}$ is the gas average velocity, F_G is gravity, F_D is the aerodynamic drag force, F_{LR} is the lift force arising from particle rotation (the Magnus lift force), ω_s is the angular velocity of a particle.

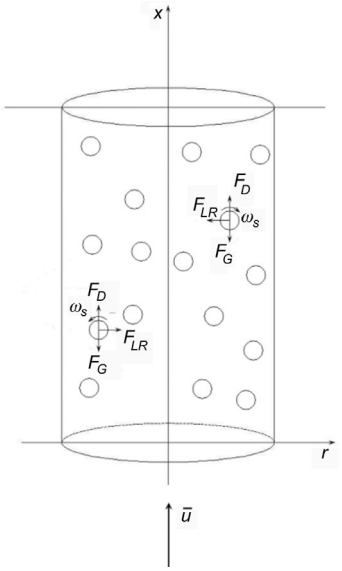

Fig. 1. Upward turbulent particulate flow in a pipe.

It is assumed that the particulate phase is polydispersed and composed of several known mass fractions. These fractions can be of single material density and characterized by equivalent particle diameter of the fraction δ. According to Kartushinsky and Michaelides (2004), in the given formulation of the governing equations that follows, three solid fractions are assumed to be present. It is assumed that the aerodynamic forces, such as the drag, lift forces, and gravity, act on all the particulate fractions.

Governing equations for the 2D RANS model

The model is based on the time-averaged Navier–Stokes equations (RANS method), without any simplifications, such as the boundary layer simplifications. The vertical pipe flows are 2D unless the study of rotating flows.

A short presentation of the governing equations written for the axisymmetric channel case is as follows.

1. Continuity equation for the gas phase:

$$\frac{\partial u}{\partial x}+\frac{\partial (rv)}{r\partial r}=0, \tag{1}$$

where u and v are the longitudinal and radial velocity components of the gas phase.

2. Longitudinal linear momentum equation for the gas phase:

$$\frac{\partial}{\partial x}\left(u^2-\tilde{\nu}_t\frac{\partial u}{\partial x}\right)+\frac{\partial}{r\partial r}r\left(uv-\tilde{\nu}_t\frac{\partial u}{\partial r}\right)=-\frac{\partial p}{\rho\partial x}+\frac{\partial}{\partial x}\tilde{\nu}_t\frac{\partial u}{\partial x}+\frac{\partial}{r\partial r}r\tilde{\nu}_t\frac{\partial v}{\partial x}-\alpha\left(\frac{u_r}{\tau'}+C_M\Omega v_r\right), \tag{2}$$

where $\tilde{\nu}_t=\nu_t+\nu$ is effective viscosity, which is the sum of turbulent and laminar viscosities, while ν_t is calculated following the Boussinesq eddy-viscosity concept; p is pressure; α is the mass concentration of particles; $u_r=u-u_s$ and $v_r=v-v_s$ are the relative velocities of particles along the longitudinal and radial directions, respectively. Here $\tau'=\tau/C'_D$ is the particle response time that specifies the drag, defined by the expression $C'_D=1+0.15\,\mathrm{Re}_s^{0.687}$ for the non-Stokesian regime (Schiller and Naumann, 1933). The particle Reynolds number and Stokesian particle response time are defined as $\mathrm{Re}_s=\delta\left|\vec{V}_r\right|/\nu=\delta\sqrt{u_r^2+v_r^2}/\nu$ and $\tau=\rho_p\delta^2/(18\rho\nu)$, respectively. $\Omega=\omega_s-0.5(\partial v/\partial x-\partial u/\partial r)$ is the angular velocity slip, with ω_s being the angular velocity of the given particle fraction. The coefficient of the Magnus lift force C_M is calculated according to Crowe et al. (1998); ρ and ρ_p are the physical densities of air and the particle material, respectively.

3. Radial linear momentum equation for the gas phase:

$$\frac{\partial}{\partial x}\left(uv-\tilde{\nu}_t\frac{\partial v}{\partial x}\right)+\frac{\partial}{r\partial r}r\left(v^2-\tilde{\nu}_t\frac{\partial v}{\partial r}\right)=-\frac{\partial p}{\rho\partial r}+\frac{\partial}{\partial x}\tilde{\nu}_t\frac{\partial u}{\partial r}+\frac{\partial}{r\partial r}r\tilde{\nu}_t\frac{\partial v}{\partial r}-\frac{2\tilde{\nu}_t v}{r^2}-\alpha\left(\frac{v_r}{\tau'}-(C_M\Omega+F_s)u_r\right), \tag{3}$$

where F_s is the coefficient for the Saffman lift force, which is due to the local shear of the flow; it is given for finite values of the particle Reynolds numbers by correction of Mei (1992).

4. Turbulence kinetic energy equation for the gas phase:

$$\frac{\partial}{\partial x}\left(uk-\tilde{\nu}_t\frac{\partial k}{\partial x}\right)+\frac{\partial}{r\partial r}r\left(vk-\tilde{\nu}_t\frac{\partial k}{\partial r}\right)=2\nu_t\left\{\left(\frac{\partial u}{\partial x}\right)^2+\left(\frac{\partial rv}{r\partial r}\right)^2+\frac{1}{2}\left(\frac{\partial u}{\partial r}+\frac{\partial v}{\partial x}\right)^2\right\}+\frac{\alpha}{\tau}(u_r^2+v_r^2+k_s)-\varepsilon_h, \tag{4}$$

where k and k_s are the turbulence kinetic energy of the gas- and dispersed phases, respectively. The hybrid dissipation rate ε_h is calculated for the two-phase flow via hybrid turbulence length scale defined as harmonic average of the integral length scale of single-phase flow and inter-particle spacing (Crowe, 2000).

5. Continuity equation for the particulate phase:

$$\frac{\partial}{\partial x}(\alpha\tilde{u}_s)+\frac{\partial}{r\partial r}r(\alpha\tilde{v}_s)=0, \tag{5}$$

where $\tilde{u}_s$ and $\tilde{v}_s$ are the longitudinal and radial components of the drift particle velocity of the given fraction, given by the expressions $\tilde{u}_s=u_s-(D_t+D_c^x)\partial\ln\alpha/\partial x$, $\tilde{v}_s=v_s-(D_t+D_c^r)\partial\ln\alpha/\partial r$. Here D_t is the coefficient of turbulent diffusion of particles, which is calculated by the model of Zaichik and Alipchenkov (2005). The pseudoviscosity diffusion coefficients along x and r directions $D_c^{x,r}$ stem from the particle collisions (Kartushinsky and Michaelides, 2004).

6. Momentum equation in the longitudinal direction for the particulate phase:

$$\frac{\partial}{\partial x}(\alpha u_s\tilde{u}_s)+\frac{\partial}{r\partial r}(r\alpha u_s\tilde{v}_s)=-\frac{\partial}{\partial x}\left(\alpha\overline{u_s'^2}\right)-\frac{\partial}{r\partial r}\left(r\alpha\overline{u_s'v_s'}\right)+\alpha\left[\frac{u_r}{\tau'}+C_M\Omega v_r-g\left(1-\frac{\rho}{\rho_p}\right)\right], \tag{6}$$

where g is gravitational acceleration.

7. Momentum equation in the radial direction for the particulate phase:

$$\frac{\partial}{\partial x}(\alpha v_s\tilde{u}_s)+\frac{\partial}{r\partial r}(r\alpha v_s\tilde{v}_s)=-\frac{\partial}{\partial x}\left(\alpha\overline{u_s'v_s'}\right)-\frac{\partial}{r\partial r}\left(r\alpha\overline{v_s'^2}\right)+\alpha\left[\frac{v_r}{\tau'}-(C_M\Omega+F_s)u_r\right], \tag{7}$$

where $\overline{u_s'^2}$, $\overline{u_s'v_s'}$, $\overline{v_s'^2}$ are the velocity correlations due to particle collisions and induce momentum swap in the longitudinal and radial motions of the given fraction (Kartushinsky and Michaelides, 2004).

8. Angular momentum equation in the longitudinal direction for the particulate phase:

$$\frac{\partial}{\partial x}(\alpha\omega_s\tilde{u}_s)+\frac{\partial}{r\partial r}(r\alpha\omega_s\tilde{v}_s)=-\frac{\partial}{\partial x}\left(\alpha\overline{u_s'\omega_s'}\right)-\frac{\partial}{r\partial r}\left(r\alpha\overline{v_s'\omega_s'}\right)-\alpha C_\omega\frac{\Omega}{\tau}, \tag{8}$$

where $\overline{u_s'\omega_s'}$ and $\overline{v_s'\omega_s'}$ are the linear-angular velocity correlations of particles due to inter-particle collisions calculated according to Kartushinsky and Michaelides (2004).

Boundary conditions for the RANS model

As inlet boundary conditions, it is assumed that particles enter the previously computed, fully developed flow domain of single phase, having the initial longitudinal velocity determined by the lag coefficient. The equilibrium outlet boundary conditions were set at the exit cross section $x=100D$, i.e. the non-gradient derivatives from all velocities of all phases, turbulence kinetic energy, and mass concentration over longitudinal coordinate were written according to Kartushinsky et al. (2009b). Since the particulate flow in the vertical pipe is considered as axisymmetrical, the non-gradient boundary conditions were set at the pipe axis for the longitudinal velocity components of gas and particles, the turbulent energy and particle mass concentration. The boundary conditions were set zero at the pipe axis for the radial velocities of both phases and the particle angular velocity. The concept of "wall functions" (Pope, 2008) has been applied to set the boundary conditions at the wall. While applying the balance of the production and dissipation rate of kinetic energy "near the wall" with using the eddy-viscosity concept (Perić and Scheuerer, 1989), it can link the friction velocity v_* and shear stress τ_w through the turbulence kinetic energy as $v_*^2=\tau_w/\rho=c_\mu^{0.5}k$. The computations near the wall were carried out at the half-width of the control volume off the

wall. Then, for the longitudinal velocity of the gas phase and for the turbulent energy computed by means of its production P_k, the boundary conditions are as follows:

$$\begin{cases} u = \sqrt{\dfrac{\tau_w}{\rho}} \dfrac{1}{æ} \ln(y^+) + C = v_* \dfrac{1}{æ} \ln\left(E \dfrac{y}{\nu} v_* \right) & 11.6 \le y^+ < 500 \\ u = \dfrac{v_*^2 y}{\nu} & y^+ < 11.6 \end{cases}, \tag{9}$$

$$P_k = \frac{2\tau_w^2}{æ \rho c_\mu^{0.25} y \sqrt{k}}, \tag{10}$$

where the empirical constant $æ = 0.41$; $y = \Delta/2$ (Δ is the width of the control volume).

The wall boundary conditions for the dispersed phase have taken into account the particle's velocity lag determined through particle–wall interaction (Kartushinsky et al., 2009b).

Numerical method

The control volume method was applied to solve mass and momentum equations of both phases by using the implicit lower and upper matrix decomposition method with flux-blending differed-correction and upwind-differencing schemes by Perić and Scheuerer (1989). Calculations were performed in dimensional form for all flow regimes. The number of the control volumes varied from 280 000 to 1 120 000, corresponding to the increase in the pipe diameter from $D = 30.5$ mm to $D = 61$ mm, and their size remained constant across the pipe flow.

RESULTS AND DISCUSSION

The numerical results presented in the figures herein have been obtained at a distance of $x/D = 100$ from the pipe entrance. At this distance it was reasonable to stipulate that the steady flow conditions had been reached and there was no influence of the entrance conditions. The results presented here are mainly dimensionless, but some of them are given in dimensional form. Coal particles 250 μm in size (physical density $\rho_p = 1600$ kg/m^3) were used in investigations. The flow mass loading was $m^* = 1$ and 10 kg dust/kg air. The applied particles were light enough to respond to turbulent fluctuations of gas.

The Reynolds number Re was assigned as the constant through all calculations and set equal to 4.4×10^4. The pipe diameter D was 30.5, 45.75, and 61 mm for the gas average velocities $\overline{u} = 21.6$, 14.6, and 10.8 m/s, respectively. The average longitudinal velocity and turbulence energy radial distributions calculated for these three regimes are shown in Figs 2 and 3.

The following figures show the influence of various force factors on radial distributions of the particle velocity lag, particle mass concentration, and turbulence modulation originating from the particles. Separately, the effects of the direct (turbulence) and indirect (no-coupling and coupling) particle–turbulence interactions are analysed, together with the singled-out influence of gravity.

The longitudinal velocity lag is presented as the ratio of the longitudinal velocity slip u_r between the gas and particulate phases to the terminal velocity of particles, $(u - u_s)/v_t$, where v_t is the particle terminal velocity.

The analysis of the behaviour of the normalized longitudinal velocity lag is shown in Fig. 4 for various force factors for 250-μm particles at $m^* = 1$. If the motion of particles is exposed only by viscous and gravitation forces (without the direct effect of turbulence, lift forces, and coupling), the velocity lag between two phases approaches the particle terminal velocity occurring in the steady-state flow domain, i.e. the ratio u_r/v_t converges to unity (the curve marked by triangles in Fig. 4). However, as the numerical simulation shows, if the motion of particles is exposed by a combined effect of various force factors, the normalized longitudinal velocity lag increases above the particle terminal velocity.

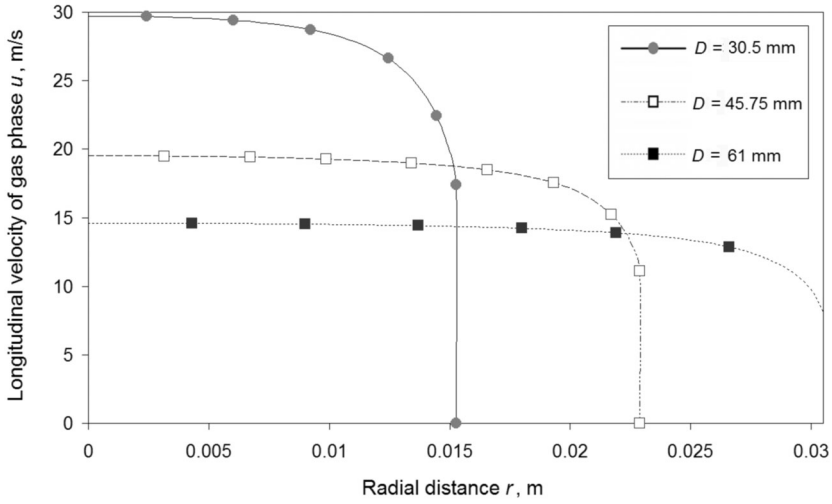

Fig. 2. Radial distributions of the longitudinal gas velocity in the pipes D = 30.5, 45.75, and 61 mm, Re = 4.4×10^4.

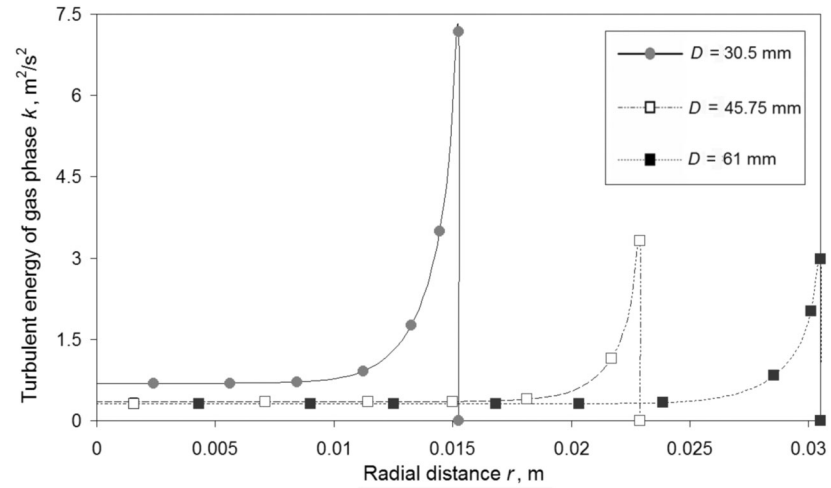

Fig. 3. Radial distributions of the turbulence energy of gas in the pipes D = 30.5, 45.75, and 61 mm, Re = 4.4×10^4.

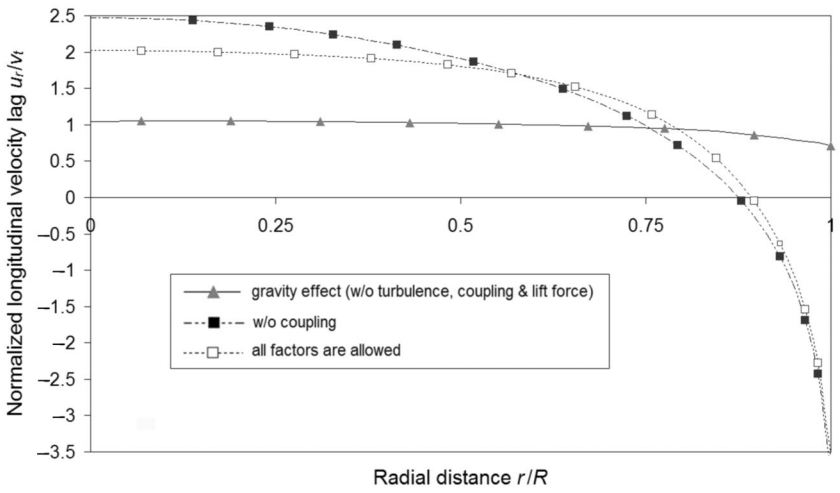

Fig. 4. Radial distributions of the normalized longitudinal velocity lag for 250 μm coal particles obtained for various flow conditions, m^* = 1, D = 45.75 mm, Re = 4.4×10^4.

Figure 5 shows the effect of the flow mass loading on the normalized longitudinal velocity lag. It is evident that increase in the flow mass loading results in reduction of u_r/v_t almost over the entire cross section of the pipe except the near-wall region.

Diminishing of the normalized longitudinal velocity lag observed for a relatively dense flow ($m^*=10$, Fig. 5) clearly depicts the tendency of turbulence attenuation by particles, or, in other words, decrease in the direct effect of turbulence on particle motion. The ratio between particle size and turbulence integral length scale is about 0.1 for the given 250-μm coal particles and, according to Gore and Crowe (1989), they attenuate turbulence. This effect becomes stronger with increase in the flow mass loading that results in the converging of u_r/v_t to unity when considering only the effect of gravity (see Fig. 4).

In order to trace the effect of the flow mass loading on turbulence modulation, let us first examine the distribution of the particle mass concentration presented in Fig. 6. As one can see, the growth of the flow mass loading attenuates turbulence and makes radial distributions steeper with a more pronounced tendency with respect to particle size variation (Kartushinsky and Michaelides, 2004, 2006).

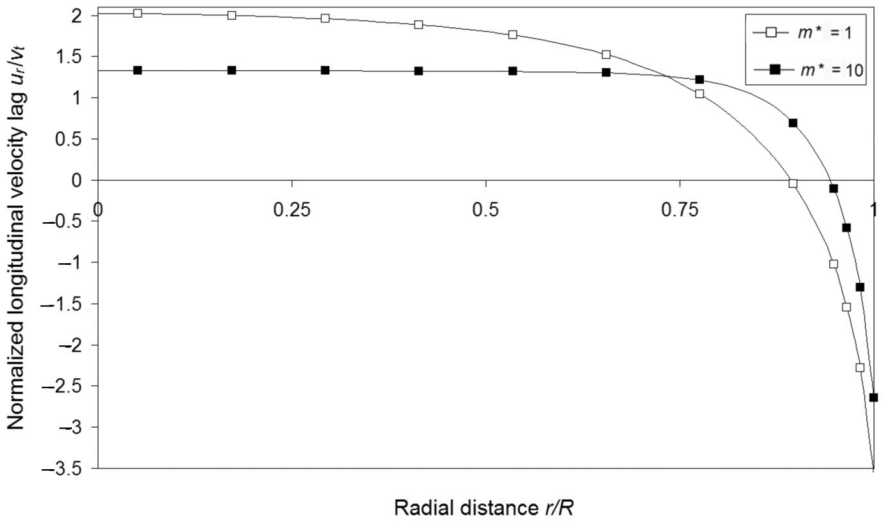

Fig. 5. Radial distributions of the normalized longitudinal velocity lag for 250 μm coal particles obtained for the flow mass loadings m^* = 1 and 10, D = 45.75 mm, Re = 4.4×10^4.

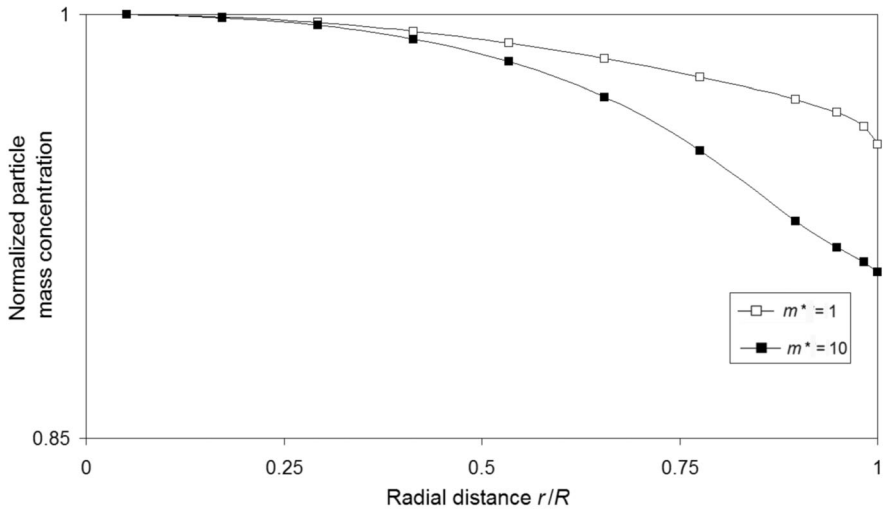

Fig. 6. Radial distributions of the normalized mass concentration of 250 μm coal particles obtained for the flow mass loadings m^* = 1 and 10, D = 45.75 mm, Re = 4.4×10^4.

Figure 7 explicitly addresses the coupling effect, which was observed for two flow mass loadings, $m^* = 1$ and 10. Obviously, a higher mass loading leads to a higher rate of turbulence modulation, i.e., if there is turbulence attenuation due to particles, this process is intensified for a higher mass loading.

The next series of plots (Figs 8–10) show the effect of the pipe diameter for a constant Reynolds number on distributions of the normalized velocity lag, particle mass concentration, and turbulence modulation.

Figure 8 shows radial distributions of the normalized longitudinal velocity lag obtained for various pipe diameters. One can see that increase in the pipe diameter results in a lower turbulence level (see Fig. 3). This, in turn, leads to a smaller velocity lag with less deviation from particle terminal velocity, and, in fact, to weaker particle involvement into the turbulent motion. This is proved by the data of Fig. 3, showing that a larger pipe diameter corresponds to a lower level of turbulence energy, and, therefore, to a lower rate of particle involvement by the gas flow.

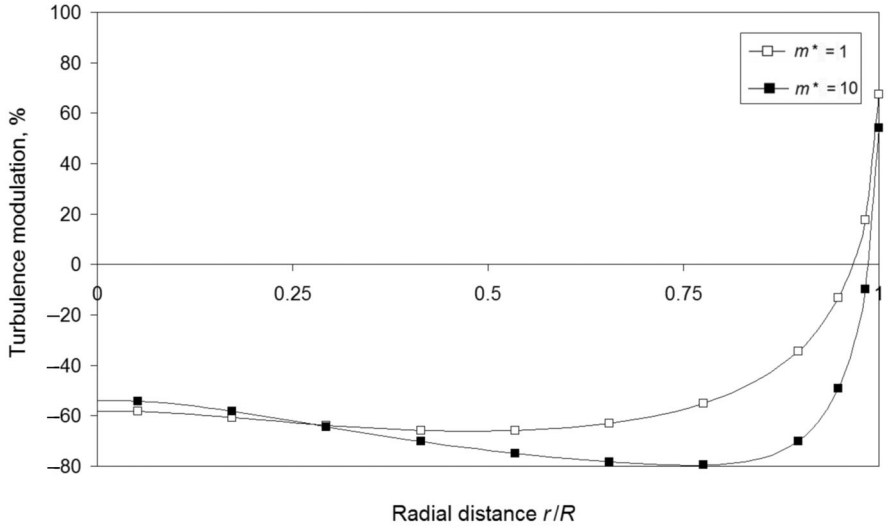

Fig. 7. Effect of mass loading on the turbulence modulation by 250 μm coal particles, $m^* = 1$ and 10, $D = 45.75$ mm, $\mathrm{Re} = 4.4 \times 10^4$.

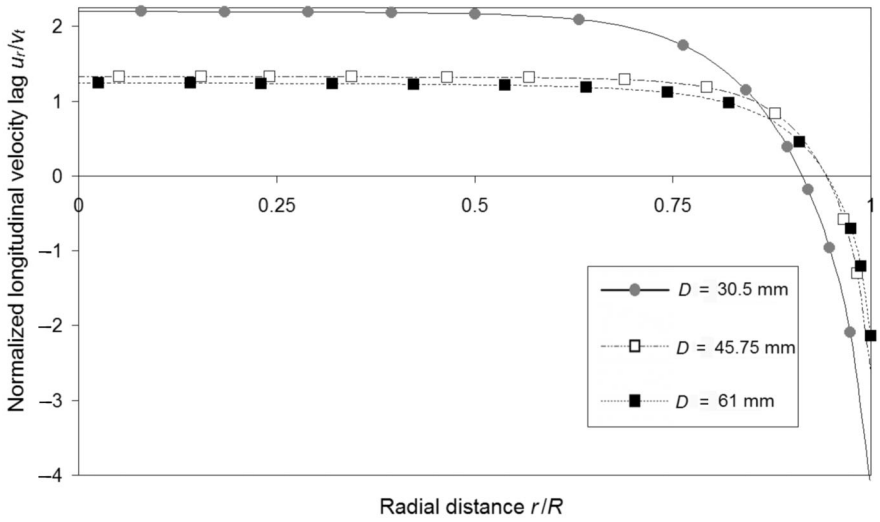

Fig. 8. Radial distributions of the normalized longitudinal velocity lag for 250 μm coal particles in the pipes $D = 30.5$, 45.75, and 61 mm, $m^* = 10$, $\mathrm{Re} = 4.4 \times 10^4$.

One can see that the effect of the pipe diameter has a tendency to straighten the radial distributions of the particle mass concentration (Fig. 9). Increase in the pipe diameter leads to reduction of the ratio between particle size and pipe diameter, which results in intensification of particle turbulent diffusion causing flattening of distributions of particle concentration (Kartushinsky et al., 2009b).

The turbulence modulation caused by particles is shown in Fig. 10 for various pipe diameters at the flow mass loading $m^* = 10$. As one can see, increase in the pipe diameter leads to a lower rate of turbulence attenuation. This can be explained based on the analysis of Fig. 3. As it shows, increase in the pipe diameter results in decrement of turbulence kinetic energy k. Since the length scale of energy-containing eddies is proportional to turbulence kinetic energy ($L_e \sim k^{\frac{3}{2}}$), the decrement of kinetic energy is followed by decrease in the turbulence length scale. This, in turn, causes the growth of the ratio between particle size and turbulence length scale, and finally results in a lower rate of turbulence attenuation due to particles.

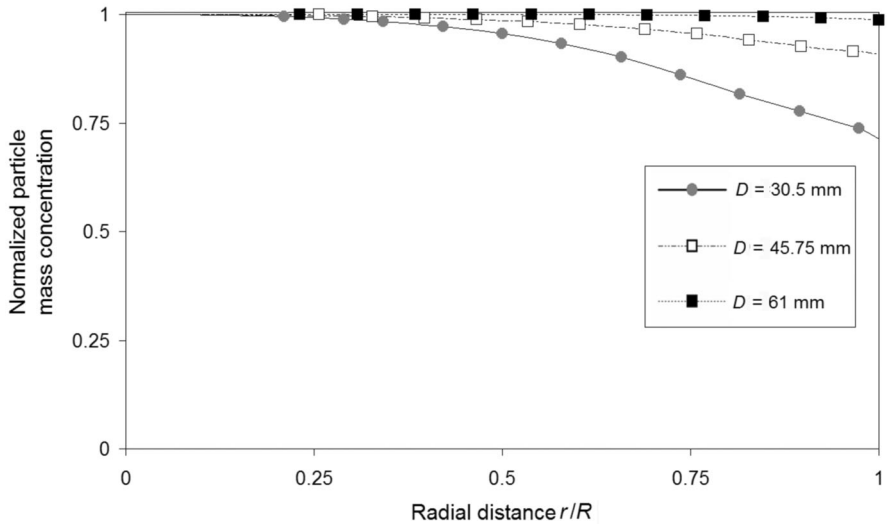

Fig. 9. Radial distributions of the normalized mass concentration for 250 μm coal particles in the pipes $D = 30.5$, 45.75, and 61 mm, $m^* = 10$, $\mathrm{Re} = 4.4 \times 10^4$.

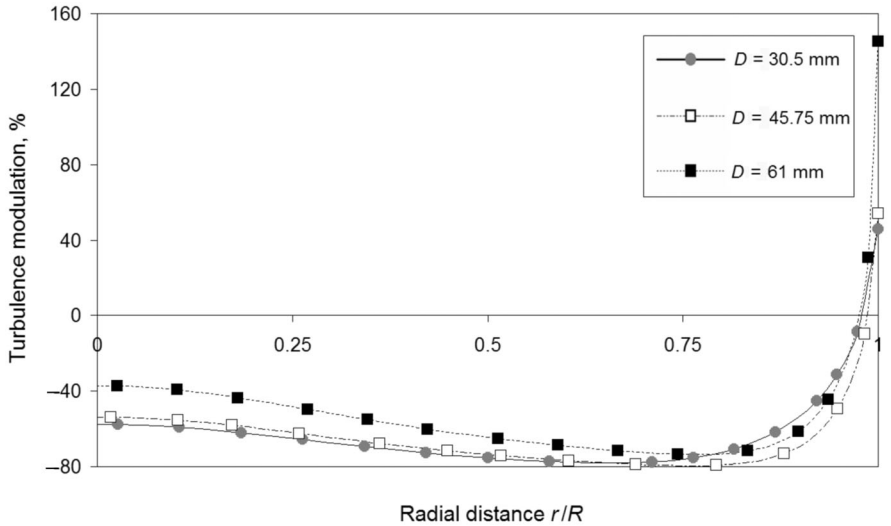

Fig. 10. Radial distributions of the turbulence modulation for 250 μm coal particles in the pipes $D = 30.5$, 45.75, and 61 mm, $m^* = 10$, $\mathrm{Re} = 4.4 \times 10^4$.

CONCLUSIONS

The two-dimensional RANS numerical approach fitted for upward turbulent particulate pipe flow supplied with the appropriate closure equations was applied to the computational investigation of parameters of gas and solid particles by the control volume method. The study covered the distance of 100 calibers from the pipe entrance.

The longitudinal velocity lag, turbulent kinetic energy of gas, and particle mass concentration, affected by gravity, viscous drag, particle–turbulence, particle–particle, and particle–wall interactions as well as the Saffman and Magnus lift forces, were examined for different pipe diameters with holding constant the flow Reynolds number for various flow mass loadings.

The obtained numerical results allow us to draw the following conclusions:

1. simultaneous effect of turbulence interactions and all force factors impacting on solid particles results in substantial excess of the longitudinal velocity lag over the terminal velocity of particles;
2. increase in the pipe diameter
   - gives rise to a decrease in the relative velocity lag,
   - flattens the radial distributions of particle velocity,
   - induces a decrease in the turbulence attenuation rate,
   - causes flattening of the radial distributions of particle mass concentration;
3. increase in the flow mass loading causes
   - decrease in the relative velocity lag,
   - increase in the rate of turbulence attenuation,
   - steepening of the radial distributions of particle mass concentration.

The presented model, with applying a minimum number of assumptions and empiricism, represents a more contemporary computational approach in turbulent particulate flow. It is also simpler and uses the state-of-the-art modelling and computational techniques, and is more accurate because it does not apply approximations. The given method allows computing large particulate flow domains occurring in various practical devices.

ACKNOWLEDGEMENTS

The work was done within the frame of targeted financing project SF0140070s08 of the Estonian Ministry of Education and Research and partially supported by the Estonian Science Foundation (grant 7620). The authors are grateful for the technical support of cluster computers at the University of Texas at San Antonio.

REFERENCES

Cabrejos, F. J. and Klinzing, G. E. 1994. Pickup and saltation mechanisms of solid particles in horizontal pneumatic transport. *Powder Technol.*, **79**, 173–186.

Cao, J. and Ahmadi, G. 1995. Gas-particle two-phase turbulent flow in vertical duct. *Int. J. Multiphase Flow*, **21**, 1203–1228.

Crowe, C. T. 2000. On models for turbulence modulation in fluid-particle flows. *Int. J. Multiphase Flow*, **26**, 719–727.

Crowe, C. T. and Gillandt, I. 1998. Turbulence modulation of fluid-particle flows – a basic approach. In *Proceedings of the 3rd International Conference on Multiphase Flow, Lyon, France, June 8–12, 1998*. CD-ROM.

Crowe, C. T., Sommerfeld, M., and Tsuji, Y. 1998. *Multiphase Flows with Droplets and Particles*. CRC Press LLC, Boca Raton, Florida.

Davies, J. T. 1987. Calculation of critical velocities to maintain solids in suspension in horizontal pipes. *Chem. Eng. Sci.*, **42**, 1667–1670.

Deutsch, E. and Simonin, O. 1991. Large eddy simulation applied to the motion of particles in stationary homogeneous fluid turbulence. In *Proceedings of the 1st ASME/JSME Fluids Engineering Conference, Portland, USA, June 23–27, 1991* (Michaelides, E. E., Fukano, T., and Serizawa, A., eds), pp. 35–42. American Society of Mechanical Engineers, New York, Series FED, **110**.

Elghobashi, S. E. and Abou-Arab, T. W. 1983. A two-equation turbulence model for two-phase flows. *Phys. Fluids*, **26**, 931–938.

Gidaspow, D. 1994. *Multiphase Flow and Fluidization: Continuum and Kinetic Theory Descriptions*. Academy Press, Boston.

Gore, R. A. and Crowe, C. T. 1989. Effect of particle size on modulating turbulent intensity. *Int. J. Multiphase Flow*, **15**, 279–285.

Kartushinsky, A. and Michaelides, E. E. 2004. An analytical approach for the closure equations of gas-solid flows with inter-particle collisions. *Int. J. Multiphase Flow*, **30**, 159–180.

Kartushinsky, A. and Michaelides, E. E. 2006. Particle-laden gas flow in horizontal channels with collision effects. *Powder Technol.*, **168**, 89–103.

Kartushinsky, A. I., Michaelides, E. E., and Zaichik, L. I. 2009a. Comparison of the RANS and PDF methods for air-particle flows. *Int. J. Multiphase Flow*, **35**, 914–923.

Kartushinsky, A. I., Michaelides, E. E., Hussainov, M. T., and Rudi, Y. 2009b. Effects of the variation of mass loading and particle density in gas-solid particle flow in pipes. *Powder Technol.*, **193**, 176–181.

Kartushinsky, A. I., Michaelides, E. E., Rudi, Y. A., Tisler, S. V., and Shcheglov, I. N. 2011. Numerical simulation of three-dimensional gas-solid particle flow in a horizontal pipe. *A.I.Ch.E. J.*, **57**, 2977–2988.

Marchioli, C., Giusti, A., Salvetti, M.-V., and Soldati, A. 2003. Direct numerical simulation of particle wall transfer and deposition in upward turbulent pipe flow. *Int. J. Multiphase Flow*, **29**, 1017–1038.

Mei, R. 1992. An approximate expression for the shear lift force on a spherical particle at finite Reynolds number. *Int. J. Multiphase Flow*, **18**, 145–147.

Michaelides, E. E. 1983. A model for the flow of solid particles in gases. *Int. J. Multiphase Flow*, **10**, 61–77.

Michaelides, E. E. 2006. *Particles, Bubbles and Drops – Their Motion, Heat and Mass Transfer*. World Scientific Publishers, New Jersey.

Perić, M. and Scheuerer, G. 1989. *CAST – A Finite Volume Method for Predicting Two-Dimensional Flow and Heat Transfer Phenomena*. GRS – Technische Notiz SRR–89–01.

Pfeffer, R., Rosetti, S., and Licklein, S. 1966. *Analysis and Correlation of Heat Transfer Coefficient and Heat Transfer Data for Dilute Gas–Solid Suspensions*. NASA Rep. TND–3603.

Pope, S. B. 2008. *Turbulent Flows*. Cambridge University Press, Cambridge – New York.

Reeks, M. W. 1992. On the continuum equations for dispersed particles in nonuniform flows. *Phys. Fluids A*, **4**, 1290–1303.

Rizk, M. A. and Elghobashi, S. E. 1989. A two-equation turbulence model for dispersed dilute confined two-phase flows. *Int. J. Multiphase Flow*, **15**, 119–133.

Schiller, L. and Naumann, A. 1933. Über die grundlegenden Berechnungen bei der Schwerkraftaufbereitung. *Z. Vereines Deutscher Ingenieure*, **77**, 318–320.

Simonin, O. 1991. Eulerian formulation for particle dispersion in turbulent two-phase flows. In *Proceedings of the 5th Workshop on Two-Phase Flow Predictions, Erlangen, Germany, March 19–22, 1990* (Sommerfeld, M. and Wennerberg, D., eds), pp. 156–166. Forschungszentrum Jülich, Jülich.

Sommerfeld, M. 2003. Analysis of collision effects for turbulent gas-particle flow in a horizontal channel. Part I: Particle transport. *Int. J. Multiphase Flow*, **29**, 675–699.

Squires, K. D. and Eaton, J. K. 1990. Particle response and turbulence modification in isotropic turbulence. *Phys. Fluids A*, **2**, 1191–1203.

Tsuji, Y. and Morikawa, Y. 1982. LDV measurements of an air-solid two-phase flow in a horizontal pipe. *J. Fluid Mech.*, **120**, 385–409.

Tsuji, Y., Morikawa, Y., and Shiomi, H. 1984. LDV measurements of an air-solid two-phase flow in a vertical pipe. *J. Fluid Mech.*, **139**, 417–434.

Yarin, L. P. and Hetsroni, G. 1994. Turbulence intensity in dilute two-phase flows. Parts I, II and III. *Int. J. Multiphase Flow*, **20**, 1–44.

Yuan, Z. and Michaelides, E. E. 1992. Turbulence modulation in particulate flows – a theoretical approach. *Int. J. Multiphase Flow*, **18**, 779–785.

Zaichik, L. I. and Alipchenkov, V. M. 2005. Statistical models for predicting particle dispersion and preferential concentration in turbulent flows. *Int. J. Heat Fluid Fl.*, **26**, 416–430.

Ülessuunatud õhktahkete osakeste toruvooluse numbriline uurimine Reynoldsi kriteeriumi konstantsetel väärtustel

Alexander Kartushinsky, Ylo Rudi, Sergei Tisler, Igor Shcheglov ja Alexander Shablinsky

Erineva läbimõõduga ülessuunatud toruvoolusi uuriti Reynoldsi meetodil keskmistatud Navieri-Stokesi telgsümmeetrilistel võrranditel põhineva numbrilise meetodiga Reynoldsi kriteeriumi konstantsetel väärtustel. Seda võtet kasutati koos sobivate sulgemisvõrranditega, mis arvestavad kõiki gaasile ja osakestele mõjuvaid jõude ning efekte: osake-osake, osake-sein, osakese-turbulentsi vastasmõjud, gravitatsioon, viskoosne kaasahaaramine ja tõstejõud. Põhivõrrandite arvuliseks lahendamiseks kasutati lõplike ruumalade tehnikat. Näidati osakeste kontsentratsiooni mõju kiiruse mahajäämuse, turbulentsi moduleerimise ja osakeste kontsentratsiooni pikiprofiilidele. Tulemuste põhjal on väidetud, et turbulentsi ja osakeste omavaheline vastasmõju suurendab faaside kiiruslikku mahajäämust, mis tuleneb turbulentsi otsesest mõjust osakeste liikumisele ning viib turbulentsitaseme vähenemisele. Osakeste kiiruse ja kontsentratsiooni pikijaotused muutuvad osakeste suuremate kontsentratsioonide juures lamedamaks.